Local magnetizations in the competing-anisotropy system $K_2Co_xFe_{1-x}F_4$: NMR investigation

W. A. H. M. Vlak
Netherlands Energy Research Foundation (ECN), P.O. Box 1, 1755 ZG Petten, The Netherlands

M. J. van Dort, A. F. M. Arts, and H. W. de Wijn
Fysisch Laboratorium, Rijksuniversiteit Utrecht, P.O. Box 80.000, 3508 TA Utrecht, The Netherlands
(Received 2 March 1988)

In the randomly mixed antiferromagnet with competing anisotropies $K_2Co_xFe_{1-x}F_4$, the temperature dependences of the magnetizations residing at Co^{2+} and Fe^{2+} are determined with ^{19}F NMR. For $x=0.27$ (oblique antiferromagnetic (OAF) phase below $T_L=27$ K) at 4.2 K, the Fe spins appear to be distributed in direction with a spread of $\pm 13°$ around a median cant angle of 42° off the c axis; the Co spins are directed at 23° with a spread of $\pm 10°$. Further, the transverse magnetization in the OAF phase is coupled with a reduction of $\langle S^z \rangle$ at both the Co and Fe sites. Molecular-field calculations reproduce these findings. For $x=0.55$ (K_2CoF_4 structure) as well as $x=0.12$ and 0.18 (K_2FeF_4 structure), the spins point along a magnetic axis to within 3°. The excitations associated with Fe, which retain a spin-wave character in the K_2FeF_4-structured systems, have energies only weakly dependent on the Co coordination.

I. INTRODUCTION

A number of experimental[1-8] and theoretical[9,10] investigations have recently been focused on the problem of randomly mixed antiferromagnets with competing anisotropies. In this paper, we present an investigation of the quasi-two-dimensional archetype of these systems, $K_2Co_xFe_{1-x}F_4$, with the aim of examining the magnetization residing at the individual Co^{2+} (effective $S_{Co}=\frac{1}{2}$) and Fe^{2+} ($S_{Fe}=2$) sites. While the end members K_2CoF_4 (Ref. 11) and K_2FeF_4 (Ref. 12), respectively, order in the axial and planar magnetic structures, the mixed system may additionally acquire the oblique antiferromagnetic (OAF) phase (cf. inset to Fig. 6).[5,6] In particular, we will consider the system with $x=0.27$, which according to neutron diffraction[5] and Mössbauer spectroscopy[7] achieves order in the axial phase at $T_N=64$ K, and enters the OAF phase at $T_L=27$ K. A preeminent probe for tracking the local magnetization in these systems is the frequency of the NMR of the ^{19}F nuclei.[13] It appears that in the OAF phase the Co and Fe spins are, even near zero temperature, inclined away from the c axis in such a way as to be left at a substantial mutual angle. In the axial and planar phases, the decrement of the local magnetization with the temperature permits us, in a number of cases, to deduce the energies of the excitations associated with the Fe spins. These energies turn out to be only weakly dependent on the composition of the first shells of neighbors.

II. EXPERIMENTAL

In Fig. 1 we present representative NMR spectra at 4.2 K, and further depict part of a quadratic layer of $K_2Co_xFe_{1-x}F_4$, identifying the nonequivalent fluorine positions. The ^{19}F nuclei at the out-of-layer F^I sites, and, for that matter, those at the in-layer F^{II} sites, primarily resonate in transferred hyperfine fields of the form $A_{19}\langle S^z \rangle$ invoked by adjacent Co^{2+} or Fe^{2+} ions. At 4.2 K, these fields amount to about 40 kG at F^I_{Fe} and 47 kG at F^I_{Co} in the axial phase; in the planar phase the hyperfine fields are about 20 and 13 kG, respectively. The dipolar contributions to A_{19} are of order 1 kG, while

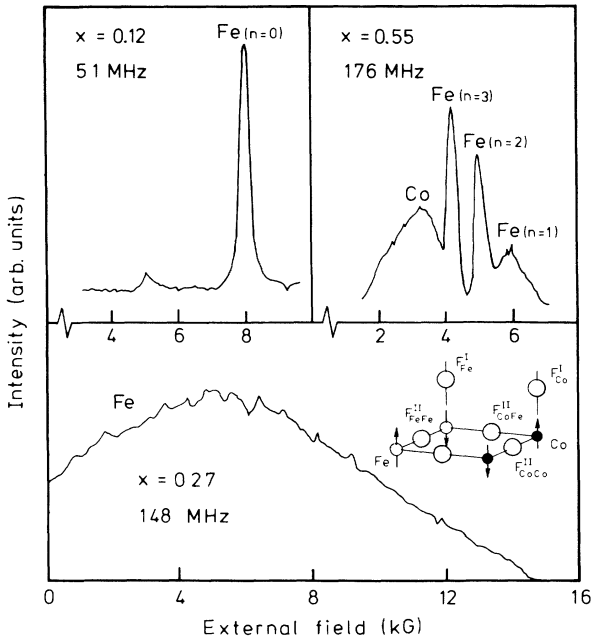

FIG. 1. Representative NMR spectra of $^{19}F^I$ adjacent to Co or Fe, with n the number of Co first neighbors, in $K_2Co_xFe_{1-x}F_4$ at 4.2 K. For $x=0.27$ and 0.55 the external field is directed along the tetragonal axis, for $x=0.12$ along an in-layer magnetic axis. The weak resonance at 5 kG for $x=0.12$ originates from F^{II}_{CoFe}. The out-of-layer F^I and in-layer F^{II} sites are identified in the inset.

more distant magnetic ions contribute by a few percent only. Small local distortions of the lattice due to the randomness, which are of order 0.01 Å,[14] induce modifications of the hyperfine constant A_{19} by several percent. These minor changes are in fact taken advantage of in that they separate the resonances, such as that of F^I adjacent to Fe^{2+} with different coordination.

Single crystals of $K_2Co_xFe_{1-x}F_4$ with $x=0.12$, 0.18. 0.27, and 0.55 were grown from the melt by Czochralski pulling, and cleaved to thin platelets of dimensions $3\times2\times1$ mm^3. The compositions x were determined with atomic absorption spectroscopy. Concentration gradients were found to be below 0.02 in x per cm. Prior to cleaving, the same crystals have been studied with neutron diffraction.[5] The specimens were aligned such that either their c axis ($x=0.27$ and 0.55) or one of the in-layer magnetic axes ($x=0.12$ and 0.18) pointed along the external field. The NMR spectrometer, employing a two-pulse spin-echo technique, was operating at fixed frequencies (50–220 MHz), the external field of typically 5 kG being swept at rates below 5 kG/min to achieve resonance. Except for $x=0.27$, all resonance frequencies have been reduced to zero external field. Here, the effects of the finite susceptibility have been ignored. Near zero temperature, the susceptibilities of Co^{2+} and Fe^{2+} predominantly are of the Van Vleck type, resulting in frequency shifts of order 30 kHz only. At 50 K, the susceptibility mainly derives from Fe^{2+},[15] and the shifts are estimated to rise to about 0.2 MHz in the fields used. A comparison of the F^I resonance frequencies of the up and down branches places an upper limit of 0.4 MHz on the susceptibility-associated shifts at 50 K. The sample temperature was maintained stable within 0.5 K. To ensure that random-field effects are absent, the ordered state was prepared by cooling in zero external field. It is noted that, once the systems are below T_N, field variations of up to 50 kG do not markedly affect the magnetic structure for all systems investigated.[16] Clearly, the systems are still far from the spin-flop transition, especially for the moderate fields used here.

The number of separate resonances observed depends on the composition x and, to some extent, the temperature. The F^I resonances may be identified according to the magnetic ion adjoining, with a further distinction according to the number n of Co^{2+} first-nearest neighbors. The former identification has been made by a comparison of the measured frequencies with the frequencies estimated from the hyperfine constants pertaining to K_2FeF_4 and K_2CoF_4. The number n of Co^{2+} neighbors then follows from the development of the frequency with temperature, upon assuming that at a given x the magnetization of the central ion drops faster, the more of its first neighbors are out of alignment with their easy axes. The identifications of n find confirmation in the relative signal intensities, which are consistent with binomial distributions appropriate to the relevant x. In a similar way, the local environments of the F^{II} have been established.

With the exception of the case $x=0.27$, the resonance lines (Fig. 1) are about 150 G in width (full width at half maximum), slightly wider than what would be expected for a composite line made up of resonances shifted by the random dipolar interactions. The additional broadening obviously originates from the inhomogeneous spread of the hyperfine parameter A_{19} due to lattice deformations and from the distribution of the local magnetizations in further-out shells.[14] As for the $x=0.27$ case, the external field was aligned along the tetragonal axis to ensure equivalence of the resonance conditions in the four domains belonging to the OAF phase. An excessive broadening of both the F^I_{Fe} and F^I_{Co} resonances is nevertheless observed below T_L (Fig. 1). This, evidently, is associated with a spread of the directions of the local magnetizations. Above T_L, where transverse critical fluctuations presumably are the primary source of the width, the resonances narrow down to about 1 kG.

III. DISCUSSION

A. $x=0.55$

We first consider the NMR data as a function of the temperature collected for $x=0.55$ (Fig. 2). The zero-field frequencies at 4.2 K are approximately 190 MHz for F^I_{Co}, 158 MHz for F^I_{Fe}, and 45 MHz for F^{II}_{CoFe}, values close to those calculated from the appropriate hyperfine constants in K_2FeF_4 (Ref. 15) and K_2CoF_4 (Ref. 17). All three resonances are split into three components, which according to the above procedure have been assigned to the Co coordinations $n=1$, 2, and 3, as indicated in Fig. 2. In the case of the somewhat broader F^I_{Co} resonance (Fig. 1), the three components are not resolved until above 40 K. To establish the directions of the magnetizations at 4.2 K to high precision, the F^I_{Fe} and F^I_{Co} resonances have been followed upon rotating the external field away from the c axis. The results, not presented in detail here, verify that both the Fe^{2+} and Co^{2+} magnetizations are aligned along the tetragonal axis to within 3°.

We now turn to the decrease of the local magnetizations $\Delta S(T)$, as reflected in the F^I frequencies $\nu(T)=\nu_0(1-\Delta S/S)$. As it appears from inspection of Fig. 2, the decrements are nearly independent of n at both the Fe and Co sites. In order to arrive at quantitative results for the energies ε of the excitations causing the drop, we have fitted the approximate expression

$$\Delta S(T)=[\exp(\varepsilon/k_BT)-1]^{-1} \quad (1)$$

to the measured temperature dependence of $\Delta S(T)$ with ε as a adjustable parameter. In Eq. (1), it is assumed that these excitations are dispersionless over a substantial part of the Brillouin zone, which is realistic in the present system. The results for ε from the three sets of F^I_{Fe} data differ only marginally. They amount to, with increasing Co coordination, $\varepsilon_{Fe(n=1)}=6.8\pm0.3$ meV, $\varepsilon_{Fe(n=2)}=7.2\pm0.3$ meV, and $\varepsilon_{Fe(n=3)}=7.7\pm0.3$ meV. Essentially the same information is contained in the F^{II}_{CoFe} data, except for a contribution due to the magnetization at the adjacent Co. Lack of precise knowledge of the relevant hyperfine parameters inhibits the separation of the Fe and Co magnetizations. Yet, the Co magnetization being virtually constant up to about 40 K, these data help to

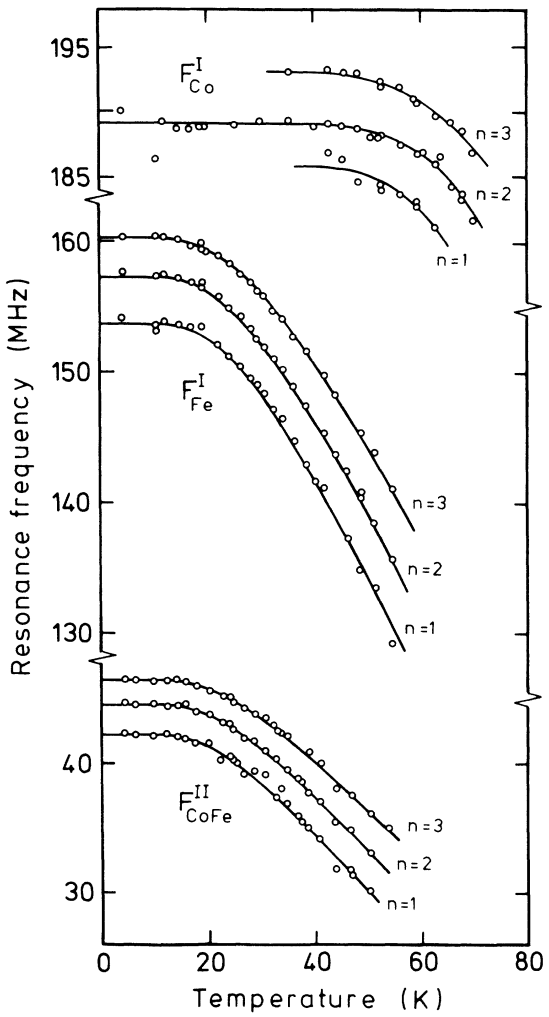

FIG. 2. ^{19}F NMR frequencies extrapolated to zero field for $x=0.55$ (transition to axial phase at 89.6 ± 0.5 K). The number of Co first neighbors is denoted by n. For F^{II}_{CoFe}, n refers to the Fe site, while the coordination of Co is 2. Curves through the data points of F^{I}_{Fe} represent fits of Eq. (1). Curves through the F^{II}_{CoFe} points are similar fits, with the NMR shift due to Co assumed constant.

refine the differences between the ε_{Fe}. Combining the F^{I}_{Fe} and F^{II}_{CoFe} data, we have $\varepsilon_{Fe(n=2)}-\varepsilon_{Fe(n=1)}=0.3\pm0.1$ meV and $\varepsilon_{Fe(n=3)}-\varepsilon_{Fe(n=2)}=0.4\pm0.1$ meV. From the F^{I}_{Co} data, we further find $\varepsilon_{Co}=27\pm5$ meV upon adopting $S=\frac{1}{2}$. The results for ε_{Fe} and ε_{Co} are in conformity with the results 8 and 32 meV determined with inelastic neutron scattering for excitations in $K_2Co_{0.6}Fe_{0.4}F_4$ in the outer part of the zone.[18] Indeed, in Eq. (1) this part carries most of the weight by virtue of the density of states, at least at the temperatures relevant to the determination of ε. The near independence of n of the local Fe^{2+} and Co^{2+} magnetizations evidently stems from the comparable sizes of the Fe-Fe, Co-Co, and Co-Fe exchange interactions. The present results, therefore, do not evidence the extent of the excitation in space, but at the Co^{2+} sites genuine localization is, of course, beyond doubt. In the diluted antiferromagnet $K_2Co_xZn_{1-x}F_4$, for comparison, the excitations residing at Co^{2+} have been found to have energies equaling multiples of $|J|$.[17]

Equation (1) is based on excitations. An alternative, equally viable, approach would be a molecular-field scaling with the host magnetization,[19] in the present case leading to the Brillouin function $B_2(S\varepsilon/k_BT)$ for $1-\Delta S(T)/S$. Like Eq. (1), the latter approach results in good fits.[20] Upon rewriting Eq. (1) to a form that better exposes the Bose ladder,

$$\Delta S(T)=\sum_{p=0}^{\infty} p\exp(-p\varepsilon/k_BT)\Big/\sum_{p=0}^{\infty}\exp(-p\varepsilon/k_BT)\ , \tag{2}$$

we see that taking the Brillouin function in place of Eq. (1) amounts to limiting the upper summation limit to $2S$. This way of writing also makes clear, first, that both approaches do not account for renormalization of the energies, nor include the zero-point spin reduction, and, second, that Eqs. (1) and (2) differ insignificantly as long as $\varepsilon\lesssim k_BT$. In effect, the differences in $\Delta S(T)$ do not exceed 1% over the range of temperatures of interest.

B. $x=0.12$ and 0.18

We now turn to the systems ordering in the planar phase. In Figs. 3 and 4 we present the temperature dependences of the NMR frequencies of F^{I}_{Fe}, F^{I}_{Co}, and F^{II}_{CoFe} for $x=0.12$ and 0.18, as far as they could be observed. As in the $x=0.55$ case, the zero-field frequencies are, within the uncertainties, in agreement with the frequencies derived from the hyperfine constants of the pure systems. Rotational diagrams again permit a refinement of the magnetic structure with respect to previous neutron-diffraction experiments,[5] specifically in the sense that Fe and Co can be examined independently. Diagrams of F^{I}_{Fe} and F^{I}_{Co} have been taken upon rotating the applied field in both the a,b and a,c planes. As an example, for $x=0.18$ the a,b diagram of F^{I}_{Fe} in the a and b domains, reflecting a perfectly tetragonal symmetry, is shown as an inset to Fig. 4. In summary of all diagrams, it is concluded that the Fe^{2+} spins and, notably enough also the Co^{2+} spins, point along the a or b magnetic axis to within 3°.

As concerns the decrement of the magnetizations with the temperature, a noteworthy feature is the close similarity with K_2FeF_4 at the Fe sites (Figs. 3 and 4).[15] Apparently, upon substituting Co for Fe to these concentrations, the excitations propagating on the Fe remain spin-wave like. This assertion is consistent with the fact that the anisotropy is on the average diminished owing to the competition between the single-ion anisotropies.[21] For a quantitative analysis of the corresponding reduction of the lower spin-wave energy gap ε_g, it seems attractive to rely on the first-order-renormalized spin-wave calculation of the sublattice magnetization in K_2FeF_4,[12] which would be adequate for the present purpose in that it accounts for the thermal decrements up to 20%. Unfortunately, in the planar phase temperature-dependent variations of the

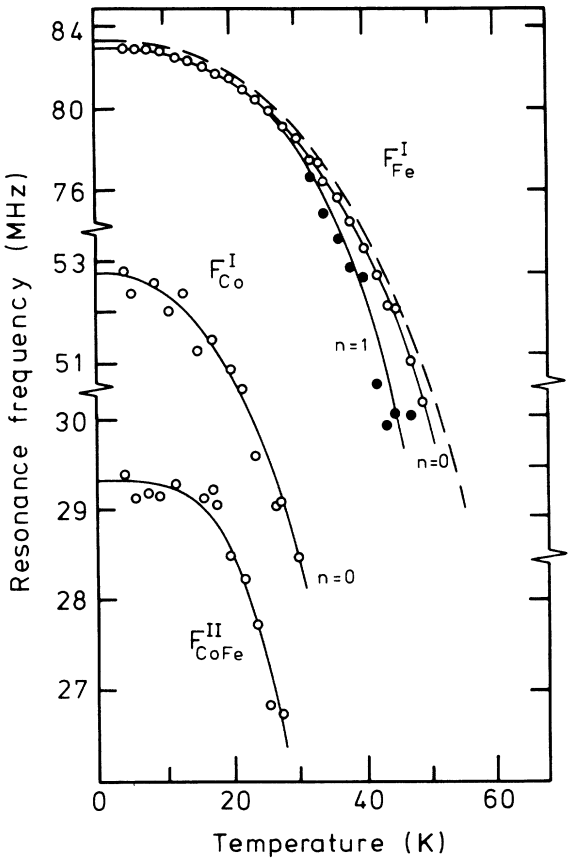

FIG. 3. ^{19}F NMR frequencies extrapolated to zero field for $x=0.12$ (transition to planar phase at 60.6±0.5 K). Dashed curve refers to K_2FeF_4 (Ref. 15).

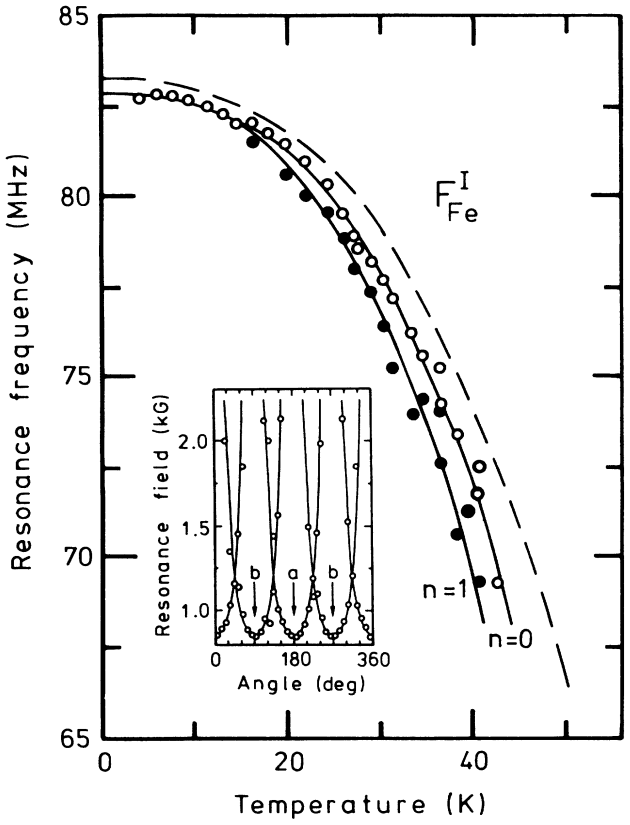

FIG. 4. Same as Fig. 3, but $x=0.18$ (transition to planar phase at 57±2 K). Solid curve in the inset, which shows the resonance field upon rotating the external field in the a,b plane, corresponds to perfectly tetragonal magnetic symmetry.

hyperfine constants, presumably invoked by magnetostriction, make the NMR overshoot the decrement of the sublattice magnetization by several percent. This was previously noticed for K_2FeF_4.[15] To circumvent these undesirable effects, we resort to a procedure in which we utilize an approximate analytical spin-wave expression of $\Delta S(T)$,[13] here adapted to K_2FeF_4, to assess the modification of ε_g with increasing x. That is,

$$\Delta S(T)\approx -\frac{1+A}{|J|S}k_BT\ln[1-\exp(-\varepsilon_g/k_BT)]\ , \quad (3)$$

in which J is the exchange parameter, and A is an anisotropy parameter defined in Ref. 12. Ignoring the variations with x of these parameters, we then find from the $F^I_{Fe(n=0)}$ data of Fig. 3 in relation to K_2FeF_4 the result $\varepsilon_g(x)/\varepsilon_g(x=0)=0.96\pm0.05$ for $x=0.12$, and similarly from Fig. 4 $\varepsilon_g(x)/\varepsilon_g(x=0)=0.85\pm0.05$ for $x=0.18$. Note that $\varepsilon_g(x=0)=2.32\pm0.10$ meV.[12] Despite the spin-wave nature of the excitations at the Fe sites, local variations in the magnetizations are manifest. In the experiments (Figs. 3 and 4), the magnetization of Fe having a single Co neighbor is observed to drop faster relative to Fe($n=0$) by about 20%. Note that the Co magnetizations, which are left transverse to the easy axis, fall even faster.

C. $x=0.27$

Finally, we discuss the NMR data recorded for the $x=0.27$ specimen. In Fig. 5 we present the temperature dependences of the external fields needed for resonances of F^I_{Co} at 200.0 MHz and F^I_{Fe} at 170.0 MHz, i.e., the hyperfine and external fields add as vectors to 49.9 and 42.5 kG, respectively. In the axial phase at 30 K, the zero-field frequency of F^I_{Co} derived from Fig. 5 is 187.0±0.5 MHz, compared to 189.9±0.5 MHz in the $x=0.55$ system at 5 K, implying virtually full alignment of the Co magnetization just above T_L. By contrast, the zero-field frequency deduced for F^I_{Fe} at 30 K, 138.2±0.5 MHz, is substantially reduced relative to the value of 158 MHz averaged over n for $x=0.55$ at 5 K. Just above T_L, therefore, the Fe magnetization is still seen to fluctuate to a substantial degree, a finding confirming the earlier combined Mössbauer and neutron-diffraction analysis.[7] Upon noting that the zero-point spin reduction is negligible in the $x=0.55$ case, we thus find the resonance frequencies $\langle S^z_{Fe}\rangle=1.75\pm0.02$ at 30 K. Similarly, at 45 K the NMR shows the Fe and Co magnetizations to be reduced relative to T_L by 14 and 4 %, respectively, both results being comparable to the $x=0.55$ case.

The data in Fig. 5 further permit, as opposed to the results from Mössbauer spectroscopy and neutron scattering, a determination of the cant angles θ the Fe and Co

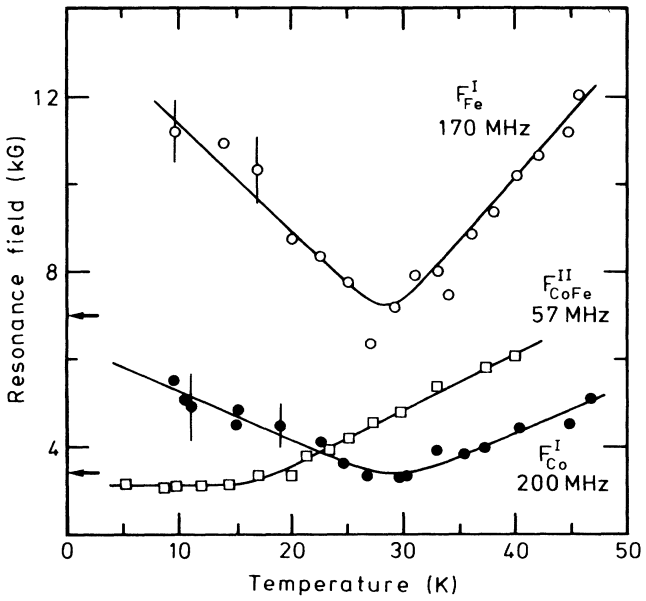

FIG. 5. External field to obtain maximum resonance signal for $x=0.27$ vs temperature (transition to axial phase at 64.4±0.5 K, and from axial to OAF phase at 27±2 K). Arrows indicate the fields expected for resonance of F^I_{Fe} and F^I_{Co} on the assumption of constancy of $\langle S^z_{Fe}\rangle$ and $\langle S^z_{Co}\rangle$ below 30 K.

spins make with the c axis, as well as their spread, at least at temperatures so low in the OAF phase that the transverse magnetizations have become saturated. We use that Fe and Co spins directed along the c axis produce hyperfine fields at the F^I nuclei at 39.5 and 47.4 kG, respectively, as derived from the appropriate zero-field zero-temperature resonance frequencies for $x=0.55$ (Fig. 2). Similarly, for alignment perpendicular to the c axis we have transverse hyperfine fields at 20.7 kG at F^I_{Fe} and 13.2 kG at F^I_{Co} from the resonance frequencies in the $x=0.12$ case (Fig. 3). Note that the hyperfine tensor in the way it is evaluated largely accounts for the effects of the dipolar fields and the zero-point spin reduction. Combining the hyperfine tensor with the external fields for resonance at 10 K, as given in Fig. 5, we then derive for the medium cant angles $\theta^{av}_{Fe}=42°\pm5°$ and $\theta^{av}_{Co}=23°\pm6°$. The former result is in accord with $\theta^{av}_{Fe}=52°\pm5°$ from Mössbauer spectroscopy at 6 K.[7] Neutron diffraction has established $\theta^{av}=28°\pm5°$ at 4.2 K for the pertinent average over the Co and Fe spins,[5] also consistent with the separate determinations of θ^{av}_{Fe} and θ^{av}_{Co} arrived at here. By similar reasoning, the spread of θ_{Fe} and θ_{Co} may be derived from the widths of the resonances (Fig. 1). From the half width at half maximum of these distributions we deduce $\Delta\theta_{Fe}=13°$ and $\Delta\theta_{Co}=10°$ to either sides of the medium angles.

The cant angles at low temperatures may alternatively be expressed in terms of spin components, resulting in $\langle S^z_{Fe}(T=0)\rangle=1.49\pm0.10$, reduced from $\langle S^z_{Fe}(T_L)\rangle=1.75\pm0.02$. Similarly, $\langle S^z_{Co}(T=0)\rangle=0.46\pm0.02$ upon adopting an effective spin $S_{Co}=\frac{1}{2}$, while $\langle S^z_{Co}(T_L)\rangle=0.50$. Mössbauer spectroscopy[7] could only marginally resolve the decrement of S^z_{Fe} upon traversing the OAF phase from T_L down to 5 K, yielding $\langle S^z_{Fe}(T=5\text{ K})\rangle/\langle S^z_{Fe}(T_L)\rangle=0.90\pm0.10$. A decrement has, within errors, not been observed with neutron diffraction.[5] To demonstrate what conclusive NMR is in establishing the reductions of the z components, we have entered in Fig. 5, as arrows, the resonance fields extrapolated from T_L to zero temperature on the assumption of constants $\langle S^z_{Fe}\rangle$ and $\langle S^z_{Co}\rangle$.

To compare the data with a model that is tractable, yet reproduces the principal features, we have elaborated upon earlier molecular-field calculations[22] by taking the nearest-neighbor configuration into account explicitly. In an iterative calculation, the equations of motion of the spins of the central ion and its four neighbors are solved numerically, upon inserting into the Hamiltonian of each spin thermodynamic averages for the components of the other spins. The further-out spins are held at the bulk molecular-field value appropriate to x and the temperature. The calculation is iterated while improving upon the thermodynamic averages after each step until self-consistency is reached. Note that the procedure implies that the modulus of each of the five spins involved is fixed to $[S(S+1)]^{1/2}$, which constitutes a coupling between S^z

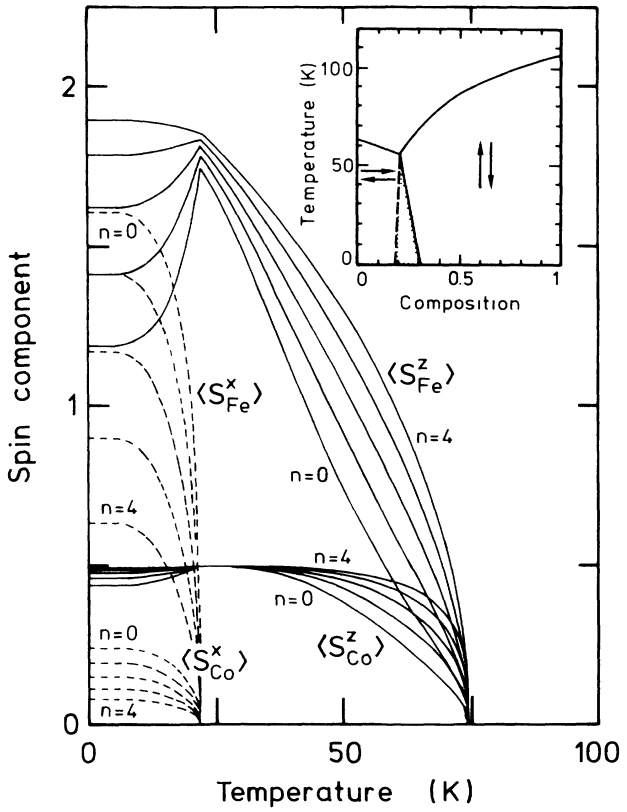

FIG. 6. Spin components of Co^{2+} and Fe^{2+} vs temperature from a mean-field calculation inclusive of the nearest-neighbor configuration for a composition corresponding to $x=0.27$. At a given temperature, $\langle S^z_{Fe}\rangle$ and $\langle S^z_{Co}\rangle$ increase with the number of Co neighbors n running from 0 to 4. Below 27 K, $\langle S^x_{Fe}\rangle$ and $\langle S^x_{Co}\rangle$ decrease with n. Inset shows the phase diagram as determined with neutron scattering (Ref. 5) and Mössbauer spectroscopy (Ref. 7).

and $S^{x,y}$. In the Hamiltonian, the Co-Co and Fe-Fe exchange interactions are taken to conform with the T_N of the end members, and the Co-Fe exchange constant is set to their geometric mean. The concentrations are finally adjusted such as to reproduce the experimental tetricritical concentration (cf. inset to Fig. 6). The results, given in Fig. 6 versus the temperature with n as parameter, account for the decrease of $\langle S^z \rangle$ below T_L. Averaging over n with weights appropriate to $x=0.27$, we find $\langle S^z_{\mathrm{Fe}}(T=0) \rangle = 1.42$, $\langle S^x_{\mathrm{Fe}}(T=0) \rangle = 1.38$, $\langle S^z_{\mathrm{Co}}(T=0) \rangle = 0.46$, and $\langle S^x_{\mathrm{Co}}(T=0) \rangle = 0.19$. For the median cant angles near 0 K we arrive at $\theta_{\mathrm{Fe}}=46°$ and $\theta_{\mathrm{Co}}=23°$ with spreads of about $\pm 10°$ and $\pm 6°$, respectively. From the model calculation it is further recovered that the magnetization in the axial phase drops the faster the larger the number of Fe neighbors in the first shell.

IV. CONCLUSIONS

With NMR the magnetizations residing at individual Fe^{2+} and Co^{2+} sites in $K_2Co_xFe_{1-x}F_4$ have been examined. As for the planar and axial phases, earlier determinations of the magnetic structure are refined. In the planar phase, the excitations primarily propagating on Fe^{2+} retain their spin-wave character, and their energy gap appears to diminish somewhat with increasing x. The energies of these excitations are only weakly dependent on the Co coordination. Of particular interest are the results for the OAF phase. Here, the spin orientations adopted by Fe^{2+} and Co^{2+} at low temperatures not only depend on the composition, but vary from site to site by as much as several tens of degrees. In our example ($x=0.27$), the cant angle at 4.2 K is distributed over $\pm 13°$ at half width around a medium angle of 42° for Fe^{2+}, and over $\pm 10°$ around 23° for Co^{2+}. The results of the mean-field calculation discussed above are in remarkable agreement with these experimental findings, as are the predictions on the cant angles provided by a recent computer simulation.[23] The NMR results have further shown $\langle S^z \rangle$ of both Fe^{2+} and Co^{2+} to reduce in conjunction with a growth of $\langle S^{x,y} \rangle$ when lowering the temperature below T_L. It should finally be emphasized that neutron diffraction, Mössbauer spectroscopy, and NMR, techniques which probe the magnetizations on different length and time scales, all have contributed to the understanding of the OAF phase.

ACKNOWLEDGMENTS

We have benefited from discussions with Dr. B. J. Dikken and Dr. E. Frikkee. One of us (M.J.v.D.) acknowledges financial support from the Netherlands Foundations Stichting voor Fundamenteel Onderzoek der Materie (FOM) and Nederlandse Organisatie voor Zuiver-Wetenschappelijk Onderzoek (ZWO).

[1] L. Bevaart, E. Frikkee, J. V. Lebesque, and L. J. de Jongh, Phys. Rev. B **18**, 3376 (1978).
[2] A. Ito, Y. Someya, and K. Katsumata, Solid State Commun. **36**, 681 (1980); A. Ito, S. Morimoto, Y. Someya, and H. Ikeda, *ibid.* **41**, 507 (1982); A. Ito, S. Morimoto, Y. Someya, Y. Syono, and H. Takei, J. Phys. Soc. Jpn. **51**, 3172 (1982).
[3] P. Wong, P. M. Horn, R. J. Birgeneau, and G. Shirane, Phys. Rev. B **27**, 428 (1983).
[4] K. Fendler, W. P. Lehmann, R. Weber, and U. Dürr, J. Phys. C **15**, L533 (1982); **17**, 4019 (1984).
[5] W. A. H. M. Vlak, E. Frikkee, A. F. M. Arts, and H. W. de Wijn, J. Phys. C **16**, L1015 (1983); Phys. Rev. B **33**, 6470 (1986).
[6] S. A. Higgins, R. A. Cowley, M. Hagen, J. Kjems, U. Dürr, and K. Fendler, J. Phys. C **17**, 3235 (1984).
[7] W. A. H. M. Vlak, B. J. Dikken, A. F. M. Arts, and H. W. de Wijn, Phys. Rev. B **31**, 4496 (1985).
[8] Po-zen Wong, Phys. Rev. B **34**, 1864 (1986).
[9] F. Matsubara and S. Inawashiro, J. Phys. Soc. Jpn. **42**, 1529 (1977); T. Oguchi and T. Ishikawa, *ibid.* **45**, 1213 (1978); Y. Someya, *ibid.* **50**, 3897 (1981).
[10] S. Fishman and A. Aharony, Phys. Rev. B **18**, 3507 (1978).
[11] H. Ikeda and M. T. Hutchings, J. Phys. C **11**, L519 (1978).
[12] M. P. H. Thurlings, E. Frikkee, and H. W. de Wijn, Phys. Rev. B **25**, 4750 (1982).
[13] H. W. de Wijn, L. R. Walker, and R. E. Walstedt, Phys. Rev. B **8**, 284 (1973).
[14] J. A. Van Luijk, A. F. M. Arts, and H. W. de Wijn, Phys. Rev. B **21**, 1963 (1980).
[15] M. P. H. Thurlings, B. J. Dikken, A. F. M. Arts, and H. W. de Wijn, Phys. Rev. B **25**, 4771 (1982).
[16] W. A. H. M. Vlak, E. Frikkee, A. F. M. Arts, and H. W. de Wijn, J. Phys. C **17**, L621 (1984).
[17] B. J. Dikken, C. Dekker, A. F. M. Arts, and H. W. de Wijn, Phys. Rev. B **32**, 5785 (1985).
[18] S. A. Higgins, R. A. Cowley, M. Hagen, J. Kjems, U. Dürr, and K. Fendler, J. Phys. C **17**, 3235 (1984).
[19] D. Hone, H. Callen, and L. R. Walker, Phys. Rev. B **144**, 283 (1966).
[20] W. A. H. M. Vlak, M. J. van Dort, A. F. M. Arts, and H. W. de Wijn, J. Magn. Magn. Mater. **54-57**, 41 (1986).
[21] S. A. Higgins, W. A. H. M. Vlak, M. Hagen, R. A. Cowley, A. F. M. Arts, and H. W. de Wijn, in *Scaling Phenoma in Disordered Systems,* edited by R. Pynn and S. Skjeltorp (Plenum, New York, 1985), p. 455; J. Phys. C **20**, 833 (1987).
[22] K. Fendler and G. von Eynatten, J. Phys. B **54**, 313 (1984).
[23] M. Hagen and S. A. Higgens, J. Phys. C **21**, 2701 (1988).